

Electrostatic interactions between graphene layers and their environment.

J. Sabio¹, C. Seoáñez¹, S. Fratini^{1,2}, F. Guinea¹, A. H. Castro Neto³, and F. Sols⁴

¹*Instituto de Ciencia de Materiales de Madrid (CSIC),
Sor Juana Inés de la Cruz 3, E-28049 Madrid, Spain*

²*Institut Néel - CNRS & Université Joseph Fourier, BP 166, F-38042 Grenoble Cedex 9, France*

³*Department of Physics, Boston University, 590 Commonwealth Av., Boston, MA 02215, USA*

⁴*Departamento de Física de Materiales, Universidad Complutense de Madrid, E-28040 Madrid, Spain.*

We analyze the electrostatic interactions between a single graphene layer and a SiO₂ substrate, and other materials which may exist in its environment. We obtain that the leading effects arise from the polar modes at the SiO₂ surface, and water molecules, which may form layers between the graphene sheet and the substrate. The strength of the interactions implies that graphene is pinned to the substrate at distances greater than a few lattice spacings. The implications for graphene NEMs, and for the interaction between graphene and a STM tip are also considered.

I. INTRODUCTION.

Graphene is a versatile two dimensional system whose electronic properties can be tuned by means of external gates.^{1,2,3} The electronic transport properties in graphene flakes on a SiO₂ substrate have been extensively studied, although the similarities and differences between these samples and graphene grown on a SiC substrate⁴ are not fully understood. The structural properties of graphene on SiO₂ are currently being investigated. STM experiments suggest that single layer graphene follows the corrugations of the SiO₂ substrate.^{5,6} Experiments on graphene NEMs indicate that the substrate induces significant stresses in few layer graphene samples.⁷ The interaction between graphene and the substrate determines the frequency of the out of plane (flexural) vibrations, which can influence the transport properties at finite temperatures.^{8,9} The interaction with the polar modes of the SiO₂ substrate gives a substantial contribution to the temperature dependence of the carrier mobility.^{10,11,12}

We analyze here different interactions between a

graphene layer, the SiO₂ substrate, and other materials which can be in the environment of the graphene layer. We consider: i) The van der Waals forces between graphene and the metallic gate below the SiO₂ substrate, ii) The electrostatic forces between the graphene layer and the polar modes of the substrate, iii) The electrostatic forces between graphene and charged impurities which may be present within the substrate and iv) The electrostatic forces between graphene and a water layer which may lay between graphene and the substrate.¹³ A sketch of the setup studied, and the different interaction mechanisms, is shown in Fig.1. We will also mention the possibility of weak chemical bonds between the graphene layer and molecules adjacent to it,^{14,15} although they will not be analyzed in detail. We do not consider a strong chemical modification of the graphene layer,^{16,17} which would change its transport properties.

The general features of the electrostatic interactions to be studied are discussed in the next section. Then, we analyze, case by case, the different interactions between the graphene layer and the materials in its environment. Section IV discusses the main implications for the structure and dynamics of graphene, with applications to graphene NEMs and the interaction between graphene and a STM tip. The last section presents the main highlights of our work.

II. ELECTROSTATIC INTERACTIONS BETWEEN A GRAPHENE LAYER AND ITS ENVIRONMENT.

The electrons in the conduction and valence band of graphene are polarized by electromagnetic potentials arising from charges surrounding it. The van der Waals interactions between metallic systems, and metals and graphene can be expressed as integrals over the dynamic polarizability of both systems, which, in turn, can be written in terms of the zero point energy of the plasmons.^{18,19} The interaction between the graphene layer and a polarizable dielectric like SiO₂ is also given by an integral of the polarizability of the graphene layer times the polarizability of the dielectric. The latter

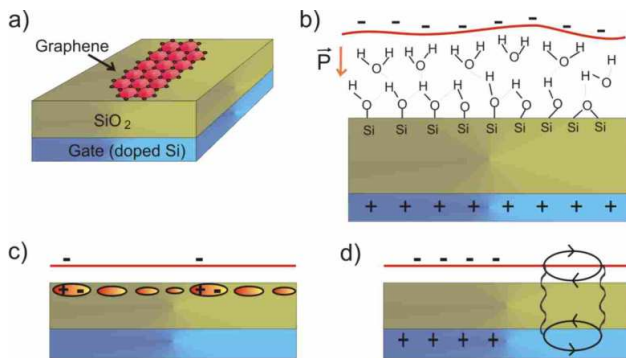


FIG. 1: a) Sketch of the system studied in the text. Interaction effects: b) Interaction with water molecules attached to hydroxyl radicals at the substrate. c) Interaction with polar modes at the surface of the substrate. d) Van der Waals interaction between the graphene sheet and the metallic gate.

can be approximated by the propagator of the polar modes, which play a similar role to the plasmons in a metal. The interaction between the graphene and static charges of electric dipoles depends only on the static polarizability.²⁰

We will calculate these interactions using second order perturbation theory, assuming a perfect graphene sheet so that the momentum parallel to it is conserved. The corresponding diagrams are given in Fig. 2. All interactions depend, on this order, linearly on the polarizability of the graphene layer. In ordinary metallic systems, the Coulomb interaction is changed qualitatively when screening by the graphene electrons is taken into account through an RPA summation of diagrams. This is not the case for undoped graphene. The Random Phase Approximation leads to a finite correction $\pi e^2/8\hbar v_F \sim 1$ to the dielectric constant, which does not change significantly the estimates obtained using second order perturbation theory.

The response function of a graphene layer at half filling is:²¹

$$\chi_G(\vec{q}, i\omega) = \frac{N_v N_s}{16\hbar} \frac{q^2}{\sqrt{v_F^2 q^2 + \omega^2}}, \quad (1)$$

where $N_s = N_v = 2$ are the valley and spin degeneracy. This expression is obtained assuming a linear dispersion around the K and K' points of the Brillouin Zone. It is valid up to a cutoff in momentum $\Lambda \sim a^{-1}$ and energy $\omega_c \sim v_F \Lambda$, where a is the lattice spacing. Beyond this scale, the susceptibility has a more complex form, and it is influenced by the trigonal warping of the bands. As Eq. (1) is scale invariant, and the electrostatic potentials to be discussed below are also scale invariant, the resulting interactions have a simple power law dependence on the distance between the graphene layer and the source of the potential. The inclusion of corrections to Eq. (1) leads to deviations from a power law dependence, which can be expressed as higher order terms which vanish as $a/z \rightarrow 0$. Hence, the calculations presented below can be considered as the lowest term in an expansion on a/z .²²

Away from half filling, the susceptibility of graphene is modified for $q \leq k_F$ and $\omega \leq \epsilon_F$.²³ The static response function goes as $\lim_{q \rightarrow 0} \chi(q, 0) \propto \epsilon_F/v_F^2$. The q component of the electrostatic potentials induced by a charge distribution at a distance z from the graphene layer decays as e^{-qz} . Hence, the momenta which contribute to the interactions between the graphene and the charge distribution are such that $q \ll z^{-1}$. The region modified by the presence of free carriers is $q \lesssim k_F$. For $z \sim 1\text{nm}$ and carrier densities such that $n \sim 10^{10} - 10^{12} \text{ cm}^{-2}$, we obtain $k_F z \sim 10^{-2} - 10^{-1}$. Hence, the corrections to the energies arising from the deviations from half filling are small, and can be obtained as an expansion on $k_F z$. In the following, we will analyze mostly the interaction energies using the expression in Eq. (1) for the graphene polarizability. The estimates presented in the next section give the leading corrections in an expansion on z^{-1} .

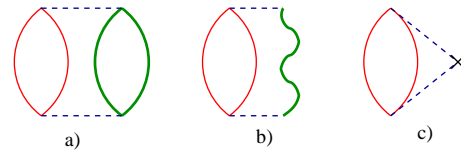


FIG. 2: Lowest order diagrams which contribute to the interaction between: a) graphene and a metal, b) graphene and a polar dielectric, and c) graphene and a static charge distribution. The thin red bubble stands for the graphene susceptibility. The thick green bubble represents the metallic susceptibility. The wavy green line stands for the propagator of a phonon mode in the dielectric. Crosses stand for static charge distributions. Dashed lines are the electrostatic potential.

We present calculations for a single layer of graphene. The energies studied here can be written as integrations over momentum space. The leading contribution comes from high momenta, $q \sim a^{-1}$. The susceptibility of multilayered samples and single graphene become small for momenta greater than $q \gtrsim t_\perp/v_F$, where t_\perp is the interlayer hopping. Neglecting the contribution from the region $q \lesssim t_\perp/v_F$, the energy of interaction between a sample made up of N graphene layers and external polarizable material is the sum of contributions of individual graphene layers. In general, the corrections induced by the interlayer hopping can be expanded in powers of $v_F/(t_\perp z)$, which, for the cases considered here, is a small parameter.

III. INTERACTIONS WITH SPECIFIC ENVIRONMENTS.

A. Metallic gate.

We describe the metallic gate as doped Si, separated from the graphene layer by a 300nm thick slab of SiO_2 dielectric. For the Si doping and voltages applied, most of the charge in the Si gate is concentrated on a layer of about 10 nm thickness,²⁴ much narrower than the distance to the graphene sheet, so that the gate is effectively two dimensional. We describe the susceptibility of the gate as that of a dirty two dimensional electron gas:

$$\chi_{gate}(\vec{q}, i\omega) = -\frac{dn}{d\mu} \frac{Dq^2}{Dq^2 + |\omega|}, \quad (2)$$

where $D = v_{Fgate} l_{gate}$ is the diffusion coefficient of the electrons in the gate, v_{Fgate} is the Fermi velocity, l_{gate} is the mean free path, and $dn/d\mu$ is the bare compressibility, given by the density of states at the Fermi level (see, for instance, Ref. 25).

The interaction between the graphene layer and the gate is given by:

$$v_q(z) = \frac{2\pi e^2}{\epsilon} \frac{e^{-qz}}{q}, \quad (3)$$

being ϵ the static dielectric constant of the SiO₂ substrate.

The lowest order contribution to the energy in perturbation theory has the following form:

$$E_{gate}^{(2)} = -\hbar \sum_q \int_0^\infty \frac{d\omega}{2\pi} v_q^2(z) \chi_G(\vec{q}, i\omega) \chi_{gate}(\vec{q}, i\omega). \quad (4)$$

For future reference, note that we use the symbol E for energies per unit area, and \mathcal{E} for total (integrated) energies. The resulting integrals can be calculated analytically in the limit $z_s \equiv D/4v_F \ll z$:

$$E_{gate}^{(2)} = -\frac{1}{12} \frac{dn}{d\mu} \frac{D}{v_F} \frac{e^4}{\epsilon^2} \frac{1}{(2z)^3} \left[\log\left(\frac{z}{z_s}\right) + \frac{1}{3} \right]. \quad (5)$$

The dependence on $z^{-3} \log(z/z_s)$ was obtained in Ref. 19.

We take, as representative parameters for the gate and the graphene layer, $D \approx 10^{-3}$ m/s, $v_F = 10^6$ m/s, $z = 300$ nm, $dn/d\mu \simeq g(E_F) = 0.04$ eV⁻¹ Å⁻² and $\epsilon = 4$ for the SiO₂ substrate. These parameters lead to interaction energies of order $\sim 10^{-8}$ meV Å⁻².

B. Polar dielectric.

The interaction between the graphene layer and the SiO₂ substrate can be expressed in terms of the electric fields induced by the surface polar modes of SiO₂.^{26,27,28,29} The coupling can be written as:

$$H_I = \sum_q M_q \rho_q (b_q + b_{-q}^\dagger), \quad (6)$$

where ρ_q is the electron density operator and b_q^\dagger, b_q the creation/destruction operators for phonons, and $M_q^2 = (\hbar^2 v_F^2) g e^{-2qz}/(qa)$ is the interaction matrix element, with g a dimensionless coupling constant. In SiO₂ we have two dominant phonon modes at $\hbar\Omega_1 = 59$ meV and $\hbar\Omega_2 = 155$ meV, with $g_1 = 5.4 \cdot 10^{-3}$ and $g_2 = 3.5 \cdot 10^{-2}$ respectively.¹¹

The lowest order contribution to the energy is given by:

$$E_{SiO_2}^{(2)} = \sum_i \sum_{\vec{q}} \int \frac{d\omega}{2\pi} \chi_G(\vec{q}, i\omega) |M_q(z)|^2 D_i^{(0)}(\vec{q}, i\omega), \quad (7)$$

where we have introduced the free phonon propagators:

$$D_i^{(0)}(\vec{q}, i\omega) = -\frac{2\Omega_i}{\omega^2 + \Omega_i^2}. \quad (8)$$

The calculation can be again carried out analytically in the limit $z \ll l_i \equiv v_F/\Omega_i$, and we obtain:

$$E_{SiO_2}^{(2)} = -\sum_i \frac{\hbar v_F}{a} \frac{g_i}{(2z)^2}, \quad (9)$$

which gives a z^{-2} dependence on the distance. Let us mention for completeness that in the opposite limit $z \gg l_i$, which is not the case of interest here, one obtains a $l_i z^{-3}$ dependence.

For $z \sim 1$ nm² and $z \gg l_i$, this term gives interaction energies of order $E_{SiO_2}^{(2)} \sim -4 \times 10^{-1}$ meV Å⁻².

C. Charges within the substrate.

In this case the calculations are done considering that effectively all the charge is concentrated close to the surface of the SiO₂ dielectric. The second order correction to the energy, averaged over the charge distribution, is:

$$E_{ch}^{(2)} = -\sum_{\vec{q}} \chi_G(\vec{q}, 0) v_q^2(z) n_{imp}, \quad (10)$$

where we consider a Coulomb interaction v_q between graphene electrons and charges that is statically screened by the effective dielectric constant at the interface, $(\epsilon + 1)/2$. Again, this contribution can be carried out analytically:

$$E_{ch}^{(2)} = -\left(\frac{2e^2}{\epsilon + 1}\right)^2 \frac{\pi n_{imp}}{2\hbar v_F} \frac{1}{2z}. \quad (11)$$

This interaction has a z^{-1} dependence, as the image potential in ordinary metals. In this case, however, this behavior arises from the combination of a vanishing density of states and lack of screening in graphene.

Reasonable values for the impurity concentration in graphene are in the range $n_{imp} \sim 10^{10} - 10^{12}$ cm⁻².^{30,31} Setting $z \sim 1$ nm, typical interaction energies are of the order $E_{ch} \sim -10^{-4} - 10^{-2}$ meV Å⁻².

D. Layer of water molecules.

The properties of the SiO₂ surface are dominated, for thermally grown SiO₂ layers, by the presence of abundant silanol (SiOH) groups,³² whose surface density is about 5×10^{14} cm⁻², unless extra steps like thermal annealing in high vacuum are taken during the fabrication process.^{33,34,35} Silanol sites are active centers for water absorption, so that the SiO₂ surface becomes hydrated under normal conditions,³⁶ which is probably the case of most of the graphene samples produced by mechanical cleavage.¹³ Moreover, several layers of water may cover the SiO₂ surface, lying between the oxide surface and the graphene samples after the graphene deposition. An analogous situation has been shown to happen in experiments with carbon nanotubes deposited on SiO₂.³⁷

The water molecule has an electric dipole, $p_w = 6.2 \times 10^{-30}$ C m ≈ 0.04 e nm. Typical fields applied in present experimental setups are $\mathcal{E} \sim 0.1$ V nm⁻¹. The energy of a water dipole when it is aligned with this field is 4 meV ~ 50 K, so that, at low temperatures, it will be oriented

along the field direction, perpendicular to the substrate and the graphene layer. For high applied electric fields, a charging of water molecules of the order $Q_{\text{H}_2\text{O}} \sim 0.1|e|$ has been reported.³⁷ The presence of these extra charges will considerably enhance the interaction between the graphene layer and the water molecules. In the following, however, we assume that the water molecules are not charged, and their dipoles are aligned perpendicular to the substrate and the graphene layer.

A water molecule which is located at a distance z from the graphene layer induces an electrostatic potential:

$$\Phi(\vec{q}, z) = 2\pi p_w e^{-|\vec{q}|z}. \quad (12)$$

This potential polarizes the graphene layer and gives rise to an interaction energy in a similar way to the static charges discussed in the preceding section. The lowest order contribution to the energy is:

$$E_{\text{water}}^{(2)} = -(ep_w)^2 \frac{\pi}{6} \frac{n_w}{\hbar v_F} \frac{1}{(2z)^3}, \quad (13)$$

where n_w is the concentration of water molecules and the z^{-3} behavior arises from the dipolar nature of the interactions. For $z = 0.3\text{nm}$, which is the approximate thickness of a water monolayer,^{38,39} the interaction energy is $E_{\text{water}}^{(2)} \sim -12n_w \text{ meV}$ which, for a typical water concentration $n_w = 10^{15}\text{cm}^{-2}$, yields $E_{\text{water}}^{(2)} \sim 1 \text{ meV}/\text{\AA}^2$.

The expression in Eq. (13) can be extended to a semi-infinite stack of water layers. For simplicity we take a distance z between graphene and the uppermost layer of water molecules equal to the interlayer distance. In this case we obtain:

$$E_{\text{water}}^{(2)} = -(ep_w)^2 \frac{\pi}{6} \frac{n_w}{\hbar v_F} \frac{\zeta(3)}{(2z)^3}, \quad (14)$$

where $\zeta(3) \approx 1.202$ is Riemann's zeta function. The present result indicates that the first water layer is the one that mostly contributes to the binding.

E. Van der Waals interaction between graphene layers.

For comparison, in this Section we evaluate the van der Waals interaction between two graphene layers at the equilibrium distance. Using the same approximations as for the other contributions, we recover the result of Ref. 19,

$$E_{G-G}^{(2)} = -\frac{\pi e^4}{16\hbar v_F} \frac{1}{(2z)^3}. \quad (15)$$

For $z = 0.3 \text{ \AA}$ this expression gives an interaction energy of $30 \text{ meV } \text{\AA}^{-2}$. This estimate is similar to other experimental and theoretical values of the graphene-graphene interaction,^{40,41} and is at least one order of magnitude greater than the other contributions analyzed earlier.

IV. ANALYSIS OF THE RESULTS.

A. Comparison of the different interactions.

Numerical estimates for the different interaction energies obtained for reasonable values of the parameters are listed in Table I. The present results show that the leading interactions are those between graphene and the polar modes of the SiO_2 substrate, and between graphene and a possible water layer on top of the substrate. Both effects are of similar order of magnitude in the present approximation, where we have assumed that the water molecules are aligned in the direction normal to the substrate.

The interactions for multi-layer graphene samples can be obtained by adding the separate contributions from each layer. The different dependences on distance imply that the relative strength of the interactions in samples with many layers can change compared to the results of Table I. For instance, the effects of the polar substrate $\propto z^{-2}$ and of charged impurities $\propto z^{-1}$, which are of longer range, sum up more effectively than the binding effect of water: the z^{-3} decay of the graphene-water interaction suggests that only the first graphene layer is affected by the presence of water on the substrate. For the same reason, the presence of several layers of aligned water molecules should not increase the binding, as only the closest layer effectively contributes to the interaction energy. On the other hand, the binding effect of water could be enhanced if the molecules were allowed to rotate freely, therefore approaching the high polarizability of liquid water,¹³ or if they were partly ionized by the applied field,³⁷ leading to additional charges similar to the Coulomb impurities present in the SiO_2 substrate.

It should be noted that we have considered here only long-range electrostatic interactions, for which reliable expressions can be obtained, in terms of well understood material parameters, like the molecular polarizability, electric dipoles, or surface modes. Still, there is a significant uncertainty in some parameters, like the distance of the relevant charges to the graphene layer and the concentration of charged impurities and water molecules. We have not analyzed the possible formation of chemical bonds between the carbon atoms and the water or silanol groups at the SiO_2 surface. Calculations based on the Local Density Functional approximation^{14,15} suggest that individual molecules can (weakly) bind to a graphene layer with energies of $10 - 50 \text{ meV}$, although it is unclear how these estimates are changed when the molecules interact at the same time with the graphene layer and the substrate.

B. Corrugation of the graphene layer induced by the substrate.

The attractive forces calculated in the preceding section imply that graphene is bound to the SiO_2 substrate,

	Distance (nm)	Dependence on distance	Energy (meV Å ⁻²)
Gate	300	$z^{-3} \log(z/z_s)$	10^{-8}
Charged impurities	1	z^{-1}	$10^{-4} - 10^{-2}$
SiO ₂ substrate	1	z^{-2}	0.4
Water molecules	0.3	z^{-3}	1
Graphene	0.3	z^{-3}	30

TABLE I: Interaction energy per unit area for the mechanisms studied in the paper. For the numerical estimates we have used typical concentrations of $10^{10} - 10^{12} \text{ cm}^{-2}$ charged impurities and 10^{15} cm^{-2} water molecules

as observed in experiments. Our previous analysis does not include the short range repulsive forces which determine the equilibrium distance. We assume that the total energy near the surface is the sum of the terms analyzed above, which have a power law dependence on the distance, and a repulsive term, $E_{rep}(z) = \epsilon_{rep}(z_0^n/z^n)$, which also decays as a power law at long distances, and z_0 is an undetermined length scale. For simplicity, we assume that the leading attractive term is due to the presence of a water layer, which behaves as $E_{water} = -\epsilon_w(z_0^3/z^3)$. The total energy per unit area is thus:

$$E(z) = \epsilon_{rep} \frac{z_0^n}{z^n} - \epsilon_w \frac{z_0^3}{z^3}. \quad (16)$$

At the equilibrium distance, z_{eq} , we have:

$$\frac{\epsilon_{rep}}{\epsilon_w} = \frac{3}{n} \left(\frac{z_{eq}}{z_0} \right)^{n-3}, \quad (17)$$

so that:

$$\begin{aligned} E''(z_{eq}) &= \frac{1}{z_{eq}^2} \left[n(n+1)\epsilon_{rep} \left(\frac{z_0}{z_{eq}} \right)^n - 12\epsilon_w \left(\frac{z_0}{z_{eq}} \right)^3 \right] \\ &= 3(n-3) \frac{\epsilon_w}{z_{eq}^2} \left(\frac{z_0}{z_{eq}} \right)^3 = 3(n-3) \frac{E_{water}(z_{eq})}{z_{eq}^2}. \end{aligned} \quad (18)$$

Hence, the order of magnitude of the pinning potential induced by the environment on the out of plane modes of graphene is given by $K \propto E_{water}(z_{eq})/z_{eq}^2 \sim 10^{-2} - 10^{-1} \text{ meV Å}^{-4}$. Defining the out of plane displacement as $h(\vec{r})$, the energy stored in a corrugated graphene layer is:

$$\mathcal{E} \approx \int d^2\vec{r} [\kappa(\Delta h)^2 + K h^2], \quad (19)$$

where $\kappa \approx 1 \text{ eV}$ is the bending rigidity of graphene.^{42,43} For modulations $h(\vec{r})$ defined by a length scale l , the bending energy dominates if $l \ll l^* = (\kappa/K)^{1/4}$, while the graphene layer can be considered rigidly pinned to the substrate if $l \gg l^*$. Using our previous estimates, we find $l^* \sim 10 \text{ Å}$, so that the graphene layer should follow closely the corrugations of the substrate.

The pinning by the substrate implies that the dispersion of the flexural modes becomes:

$$\omega_k = \sqrt{\frac{K}{\rho} + \frac{\kappa k^4}{\rho}} \quad (20)$$

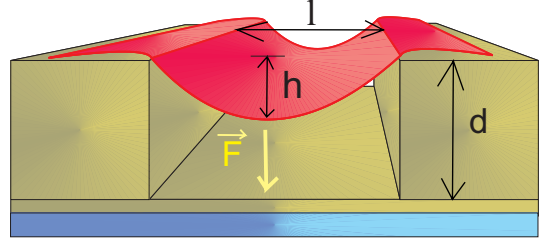


FIG. 3: Sketch of the deformation of a NEM device studied in the text.

where ρ is the mass density of the graphene layer. At long wavelengths, $\lim_{k \rightarrow 0} \omega_k = \omega_0 \sim 10^{-4} - 10^{-3} \text{ meV} \sim 10^{-3} - 10^{-2} \text{ K}$.

The estimates obtained above also allow us to analyze the bending of graphene NEMs due to the interaction with the material below, at distance d .^{7,44} We assume that the lateral dimension of the graphene cantilever is l . The maximum displacement of the graphene layer from a flat position is h . A sketch of the graphene cantilever is shown in Fig.3. We consider the force induced by charges in the substrate below the cantilever, as this is the contribution which decays more slowly as function of the distance between the graphene layer and the substrate (see Table I). If the distance of the cantilever to the substrate is d , and supposing $d \gg h$, the gain in energy due to the deformation of the graphene layer is $\mathcal{E} \sim \epsilon_{ch} l^2 z_0 h d^{-2}$, where we have again defined z_0 and ϵ_{ch} through $E_{ch}(d) = \epsilon_{ch} z_0/d$, having $\epsilon_{ch} \sim 0.1 \text{ meV Å}^{-2}$ and $z_0 \sim 1 \text{ nm}$ from our estimates of Sec. III C. This energy should compensate the elastic energy associated to the deformation, $\mathcal{E}_{el} \sim \kappa h^2/l^2$. Finally, we find:

$$h \sim \frac{\epsilon_{ch} z_0}{\kappa} \frac{l^4}{d^2} \sim 10^{-4} \text{ Å}^{-1} \frac{l^4}{d^2} \quad (21)$$

For structures such that $l \sim d$, this estimate suggests that the graphene layer will be significantly deformed if $l \gtrsim 100 \text{ nm}$.

C. Interaction with a metallic tip in an STM experiment

It is known that STM tips on graphite surfaces sometimes deform the surface graphene layer,^{45,46} and the understanding of these deformations can be of interest for current research on graphene.^{5,6,47} The analysis of the electrostatic interactions between a graphene layer and its environment allows us to estimate possible deformations induced by an STM tip. We analyze the setup sketched in the inset of Fig.4. The tip has lateral dimension l and it is located at a distance d from a graphene layer. This graphene layer interacts with an underlying substrate, and a voltage V is applied between the graphene layer and the tip. We consider three interactions:

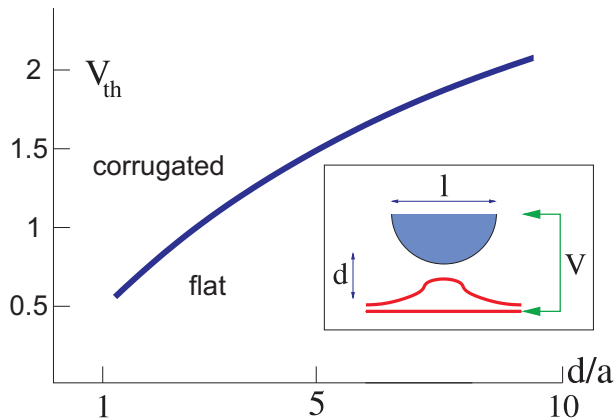


FIG. 4: Estimate of the threshold voltage as function of graphene-tip separation needed to detach a graphene layer from the substrate. The inset shows a sketch of the geometry considered in the text.

i) An attraction between the tip and the graphene layer, which tends to deform the graphene, in the way shown in Fig.4. We assume that this energy is purely electrostatic. A simple estimate can be obtained by describing the setup as a capacitor where the area of the plates is l^2 , the distance between the plates is d , and the applied voltage is V . The interaction energy is of the order:

$$\mathcal{E}_{G-tip} \approx \frac{V^2 l^2}{8\pi e^2 d}, \quad (22)$$

where we define V in energy units.

ii) The pinning of the graphene layer to the substrate. This contribution opposes the deformation of the layer. We write it as:

$$\mathcal{E}_{pin} \approx \epsilon_{pin} l^2, \quad (23)$$

where ϵ_{pin} is the pinning energy per unit area. As typical values, we will use $1 \text{ meV}/\text{\AA}^2$ for graphene on a water layer, and $30 \text{ meV}/\text{\AA}^2$ for graphene interacting with another graphene layer, as in graphite.

iii) The rigidity of the layer against flexural deformations. This term tends to keep the layer flat. The deformed region is likely to be (at least) as large as the size of the STM tip. As a result, an upper bound to the energy stored in a deformation is:

$$\mathcal{E}_{el} \approx \kappa \frac{d^2}{l^2} \quad (24)$$

The graphene layer will be deformed when:

$$\mathcal{E}_{G-tip} \gtrsim \mathcal{E}_{pin} + \mathcal{E}_{el}. \quad (25)$$

Note that the approximations involved in obtaining the various terms are valid only if $d \gtrsim a$.

We consider a situation where ϵ_{pin}, κ and l are fixed. Eq.(25) implies that the layer is deformed if the voltage exceeds a threshold:

$$V \gtrsim V_{th}(d) \approx \sqrt{8\pi \left(\frac{\kappa e^2 d^3}{l^4} + \epsilon_{pin} e^2 d \right)} \quad (26)$$

Assuming $l \sim 10a$ and $d \sim a$, we see that the dominant contribution comes from the pinning term Eq. (23). Hence, in the physically relevant range $a \lesssim d \ll l$, we can write:

$$V_{th}(d) \approx \sqrt{8\pi \epsilon_{pin} e^2 d}, \quad (27)$$

independent on the tip size. The threshold values for graphene on SiO_2 are of about 0.5-2 V for $d \sim 1 - 10 \text{\AA}$, as schematically shown in Fig.4.

V. CONCLUSIONS.

We have analyzed the electrostatic interactions between a graphene layer and the polarizable materials which may be present in its environment, for samples deposited on SiO_2 . The strength of these interactions can be obtained in terms of a few well understood microscopic parameters, and they have a simple dependence on the distance between the graphene layer and the system which induces the electrostatic field. The analysis presented here should give reliable estimates of the order of magnitude of the different interactions, and of their relative strength. We have not considered the possible formation of chemical bonds, which may alter the results when the distances between the carbon atoms in the graphene layer and the surrounding materials is sufficiently small.

We find that the leading effects arise from the polar modes of the SiO_2 substrate, and water which may form layers on top of it. Table I presents the main results. The interaction energies with systems with N layers can be obtained, to a first approximation, by adding the contributions from each layer.

The strength of the interactions suggests that a single graphene layer is pinned to the substrate on length scales greater than a few lattice spacings, $\sim 10 \text{\AA}$. This interaction modifies the long wavelength, out of plane flexural modes, which acquire a finite frequency, $\omega_0 \sim 10^{-4} - 10^{-3} \text{ meV}$. The long range forces considered here can also induce large deformations in graphene NEMs. Besides, we have analyzed the possibility of deformations of the graphene layer by an STM tip. We find that a voltage drop of 0.5 - 2 V between the tip and the sample at distances 1 - 10 \AA is sufficient to deform the graphene layer.

VI. ACKNOWLEDGEMENTS.

This work was supported by MEC (Spain) through grant FIS2005-05478-C02-01, the Comunidad de Madrid,

through the program CITECNOMIK, CM2006-S-0505-ESP-0337, the European Union Contract 12881 (NEST) (J. S., C. S., S. F., and F. G.), MEC through grant FIS2004-05120 and FIS2007-65723, and EU Marie Curie RTN Programme no. MRTN-CT-2003-504574 (F.S. and J.S.). A. H. Castro Neto was supported through the NSF grant DMR-0343790. J. S. acknowledges the I3P

Program from CSIC, and C.S. the FPU Program from MEC, for funding. We are thankful to A. Bachtold and A. K. Geim for many helpful insights into the relevance of water for current experiments, and to S. Vieira for useful information on the interaction between graphene and STM tips.

-
- ¹ K. S. Novoselov, D. Jiang, F. Schedin, T. J. Booth, V. V. Khotkevich, S. V. Morozov, and A. K. Geim, *Proc. Nat. Acad. Sc.* **102**, 10451 (2005).
- ² A. K. Geim and K. S. Novoselov, *Nature Materials* **6**, 183 (2007).
- ³ A. H. Castro Neto, F. Guinea, N. M. R. Peres, K. S. Novoselov, and A. K. Geim (2007), arXiv:0709.1163.
- ⁴ C. Berger, Z. M. Song, T. B. Li, X. B. Li, A. Y. Ogbazghi, R. Feng, Z. T. Dai, A. N. Marchenkov, E. H. Conrad, P. N. First, et al., *J. Phys. Chem. B* **108**, 19912 (2004).
- ⁵ M. Ishigami, J. Chen, W. Cullen, M. Fuhrer, and E. Williams, *Nano Lett.* **7**, 1643 (2007).
- ⁶ E. Stolyarova, K. T. Rim, S. Ryu, J. Maultzsch, P. Kim, L. E. Brus, T. F. Heinz, M. S. Hybertsen, and G. W. Flynn, *Proc. Natl. Acad. Sci. USA* **104**, 9209 (2007).
- ⁷ J. S. Bunch, A. M. van der Zande, S. S. Verbridge, I. W. Frank, D. M. Tanenbaum, J. M. Parpia, H. G. Craighead, and P. L. McEuen, *Science* **315**, 490 (2007).
- ⁸ M. I. Katsnelson and A. K. Geim (2007), arXiv:0706.2490.
- ⁹ S. Morozov, K. S. Novoselov, M. I. Katsnelson, F. Schedin, D. Elias, J. A. Jaszczak, and A. K. Geim (2007), arXiv:0710.5304.
- ¹⁰ A. G. Petrov and S. V. Rotkin, *JETP Letters* **84**, 156 (2006).
- ¹¹ S. Fratini and F. Guinea (2007), arXiv:0711.1303.
- ¹² J. H. Chen, C. Jang, S. Xiao, M. Ishigami, and M. S. Fuhrer (2007), arXiv:0711.3646.
- ¹³ F. Schedin, A. K. Geim, S. V. Morozov, D. Jiang, E. H. Hill, P. Blake, and K. S. Novoselov, *Nature Mat.* **6**, 652 (2007).
- ¹⁴ O. Leenaerts, B. Partoens, and F. M. Peeters (2007), arXiv:0710.1757.
- ¹⁵ T. O. Wehling, K. S. Novoselov, S. V. Morozov, E. E. Vdovin, M. I. Katsnelson, A. K. Geim, and A. I. Lichtenstein (2007), arXiv:cond-mat/0703390.
- ¹⁶ T. J. Echtermeyer, M. C. Lemme, M. Baus, B. N. Szafrank, A. K. Geim, and H. Kurz (2007), arXiv:0712.2026.
- ¹⁷ X. Wu, M. Sprinkle, L. X. F. Ming, C. Berger, and W. A. de Heer (2007), arXiv:0712.0820.
- ¹⁸ S. L. Tan and P. W. Anderson, *Chem. Phys. Lett.* **97**, 23 (1983).
- ¹⁹ J. F. Dobson, A. White, and A. Rubio, *Phys. Rev. Lett.* **96**, 073201 (2006).
- ²⁰ For a metal, this interaction can be written as the interaction between the charge distribution and its image.
- ²¹ J. González, F. Guinea, and M. A. H. Vozmediano, *Nucl. Phys. B* **424**, 596 (1994).
- ²² A polar dielectric introduces new length scales, $l_i = v_F/\Omega_i$ associated to the frequencies of its normal modes, Ω_i , see next section.
- ²³ B. Wunsch, T. Stauber, F. Sols, and F. Guinea, *New J. Phys.* **8**, 318 (2006).
- ²⁴ S. Sze, *Physics of semiconductor devices* (Wiley-Interscience (New York), 1981).
- ²⁵ F. Guinea, R. A. Jalabert, and F. Sols, *Phys. Rev. B* **70**, 085310 (2004).
- ²⁶ J. Sak, *Phys. Rev. B* **6**, 3981 (1972).
- ²⁷ S. Q. Wang and G. D. Mahan, **6**, 4517 (1972).
- ²⁸ N. Mori and T. Ando, *Phys. Rev. B* **40**, 6175 (1989).
- ²⁹ I. N. Hulea, S. Fratini, H. Xie, C. L. Mulder, N. N. Iosad, G. Rastelli, S. Ciuchi, and A. F. Morpurgo, *Nature Materials* **5**, 982 (2006).
- ³⁰ K. Nomura and A. H. MacDonald, *Phys. Rev. Lett.* **98**, 076602 (2007).
- ³¹ S. Adam, E. H. Hwang, V. M. Galitski, and S. Das Sarma (2007), arXiv:0705.1540.
- ³² B. Morrow and A. McFarlan, *J. Non-Crys. Sol.* **120**, 61 (1990).
- ³³ O. Snih and S. George, *J. Phys. Chem.* **99**, 4639 (1995).
- ³⁴ Y. Dong, S. Pappu, and Z. Xu, *Anal. Chem.* **70**, 4730 (1998).
- ³⁵ J. Nawrocki, *J. Chromatogr.* **779**, 29 (1997).
- ³⁶ A. M. Botelho do Rego and L. F. Vieira Ferreira (Academic Press, New York, 2001), vol. 2 of *Handbook of surfaces and interfaces of materials*, p. 275.
- ³⁷ W. Kim, A. Javey, O. Vermesh, Q. Wang, Y. Li, and H. Dai, *Nano Lett.* **3**, 193 (2003).
- ³⁸ M. Antognozzi, A. Humphris, and M. Miles, *Appl. Phys. Lett.* **78**, 300 (2001).
- ³⁹ A. Opitz, M. Scherge, S.-U. Ahmed, and J. Schaefer, *J. Appl. Phys.* **101**, 064310 (2007).
- ⁴⁰ L. X. Benedict, N. G. Chopra, M. L. Cohen, A. Zettl, S. G. Louie, and V. H. Crespi, *Chem. Phys. Lett.* **286**, 490 (1998).
- ⁴¹ M. Hasegawa, K. Nishidate, and H. Iyetomi, *Phys. Rev. B* **76**, 115424 (2007).
- ⁴² E.-A. Kim and A. H. Castro Neto (2007), arXiv:cond-mat/0702562.
- ⁴³ E. Marinari and F. von Oppen (2007), arXiv:0707.4350.
- ⁴⁴ C. Seoáñez, F. Guinea, and A. H. Castro Neto, *Phys. Rev. B* **76**, 125427 (2007).
- ⁴⁵ J. P. Batra, N. García, H. Rohrer, H. Salemkink, E. Stoll, and S. Ciraci, *Surf. Sci.* **181**, 126 (1987).
- ⁴⁶ M. Salmeron, D. F. Ogletree, C. Ocal, H. C. Wang, G. Neubauer, W. Kolbe, and G. Meyers, *Journ. Vac. Sci. and Tech.* **9**, 1347 (1991).
- ⁴⁷ G. Li and E. Y. Andrei, *Nature Phys.* **3**, 623 (2007).